Physics of the Earth and Planetary Interiors 257 (2016) 149–157

Contents lists available at ScienceDirect

Physics of the Earth and Planetary Interiors

journal homepage: www.elsevier.com/locate/pepi

A new database of source time functions (STFs) extracted from the SCARDEC method

Martin Vallée *, Vincent Douet

Institut de Physique du Globe de Paris, Sorbonne Paris Cité, Université Paris Diderot, CNRS, Paris, France

ARTICLE INFO

Article history:
Received 21 December 2015
Received in revised form 16 May 2016
Accepted 17 May 2016
Available online 03 June 2016

Keywords:
Source time function
Source parameters
Global seismicity
Tectonics
Subduction

ABSTRACT

SCARDEC method (Vallée et al., 2011) offers a natural access to the earthquakes source time functions (STFs), together with the 1st order earthquake source parameters (seismic moment, depth and focal mechanism). This article first aims at presenting some new approaches and related implementations done in order to automatically provide broadband STFs with the SCARDEC method, both for moderate and very large earthquakes. The updated method has been applied to all earthquakes above magnitude 5.8 contained in the NEIC-PDE catalog since 1992, providing a new consistent catalog of source parameters associated with STFs. This represents today a large catalog (2782 events on 2014/12/31) that we plan to update on a regular basis. It is made available through a web interface whose functionalities are described here.

1. Introduction

Earthquake moment rate functions – often referred as source time functions (STFs) – offer an integrated view of the seismic source process. Their duration and their peak value are used to infer the global earthquake characteristics and in particular the stress or strain drop (Bilek and Lay, 1999; Houston, 2001; Tocheport et al., 2007; Vallée, 2013). Compared to corner frequency measurements (Brune, 1970; Boatwright, 1984; Allmann and Shearer, 2009), STF are richer as they contain the broad-band spectrum of the source process. As such, they can be used to calculate the radiated energy (Vassiliou and Kanamori, 1982), and to explore how the source spectrum behaves with respect to theoretical models (for example the omega-square model, Aki, 1967, 1972). Observations of STFs are therefore an efficient tool to quickly determine abnormal earthquakes such as the tsunami earthquakes, that are strongly depleted in high frequencies (Kanamori, 1972). From a practical point of view, their properties can also be studied to understand the influence of the seismic source on the strong ground motions generated by earthquakes (Margaris and Hatzidimitriou, 2002; Baltay et al., 2013; Cotton et al., 2013; Courboulex et al., 2016). Finally, STFs are more and more used in tomographic studies, as recent approaches aims at fitting the waveforms for periods close to the source duration (Sigloch and Nolet, 2006; Stähler and Sigloch, 2014; Garcia et al., 2013; Hosseini and Sigloch, 2015).

STFs are closely related to the seismic waves observed at teleseismic distances. In an infinite non-attenuating medium and for a point source representation, STFs are directly the P or S waveforms scaled by a factor depending on the radiation pattern, the distance and the elastic properties. The more realistic configuration of an extended source in a spherical Earth adds some complexities to the STF extraction, in particularly when the earthquake is shallow, which leads to wave interferences between direct waves (P or S) and surface reflected phases (pP, sP, sS...). In this case, STF has to be determined together with focal mechanism and earthquake depth. The source extent also has the consequence that each seismic station and wave type (P or S) theoretically provide a different estimate of the STF (called apparent source time function, or ASTF). However, when using P waves, this effect is modest, except for very long and fast-propagating earthquakes, and the ASTF extracted from a given station gives a good estimate of the STF.

Thanks to this close link with the observed seismograms, STFs are known to be one of the most robust characterizations of the source process, and have the potential to be provided routinely. However, a global catalog of STFs – similar to what GCMT provides for the 1st order source parameters (Ekström et al., 2012) – does not exist today, although several groups are building STF catalogs for specific applications (Stähler and Sigloch, 2014; Garcia et al., 2013; Hosseini and Sigloch, 2015). Up to now, only Tanioka and Ruff (1997) followed this direction of making available their derived STFs through the Michigan STF catalog. This catalog was containing a number of STFs for earthquakes of the 1990s and

* Corresponding author.
E-mail address: vallee@ipgp.fr (M. Vallée).

http://dx.doi.org/10.1016/j.pepi.2016.05.012
0031-9201/

beginning of the 2000s but does not appear to have been updated since.

A recent approach, called SCARDEC (Vallée et al., 2011), is able to provide routinely the STF, together with the 1st order earthquake characteristics (seismic moment, focal mechanism and depth). This method has been validated on large earthquakes with independent techniques and wave types (Lentas et al., 2013) and first examples of exhaustive analyses of the SCARDEC STFs can be found in Vallée (2013) and Courboulex et al. (2016). Recent automatic solutions can be seen on the GEOSCOPE website (http://geoscope.ipgp.fr/index.php/en), where a near-real time solution is provided about 45 min after an earthquake of magnitude larger than 5.5–6.

In this article, we first provide the main steps that have been followed to extract the STFs, with an emphasis on the points which have not been explicitly described in the original SCARDEC article (Vallée et al., 2011). The characteristics of the STF catalog – which also offers independent estimates for magnitude, depth, focal mechanism for each earthquake – are then discussed, and we also underline some precautions that should be taken when using the STFs. Finally, we describe the functionalities of the web request tool providing public access to the whole catalog (in 2015, about 2800 STFs for earthquakes with occurrence posterior to 1992).

2. Exhaustive extraction of STFs from the SCARDEC method

We describe here the main steps which have been followed to extract the STFs of the present catalog. Most of the specifics have been described in the article of Vallée et al. (2011), where the SCARDEC method has been introduced. SCARDEC deconvolutive method uses the teleseismic body waves (P and SH, but also PP, PcP, and ScSH) recorded at the global stations of the Federation of Digital Seismograph Networks (FDSN) to determine the earthquake source parameters (double couple focal mechanism, moment magnitude, depth and STF). Teleseismic phases are modeled with an approach combining the reciprocity theorem and the reflectivity method (Bouchon, 1976; Müller, 1985), in the IASP91 Earth model (Kennett and Engdahl, 1991). Mantle attenuation is taken into account through a frequency dependent t^* operator. This is motivated by the fact that constant t^* values of the order of 1 s (as the one deduced from PREM; Dziewonski and Anderson, 1981) lead to an underestimation of the P-wave high frequency content (e.g. Der, 1998). This frequency dependency is here modeled by $t^*(f) = 0.39 \cdot f^{-0.25}$ (for a discussion on the frequency dependent t^*, see Choy and Cormier, 1986; Anderson and Minster, 1979), which implies for example $t^*(0.01) = 1.24$ s, $t^*(0.1) = 0.7$ s and $t^*(3) = 0.3$ s. Fig. 1 shows how the SCARDEC method has been extended here in order to (1) analyze earthquakes over the broad magnitude range M = [5.8–9] and (2) automatically extract optimal and average STFs from the ASTFs.

In order to guarantee the stability of the SCARDEC method, an important point is a first-order knowledge of the source duration (named T_d in Fig. 1). When the earthquake is large, typically larger than magnitude 7, this information can be obtained from the P waves records filtered around 1 Hz (e.g. Ni et al., 2005; Vallée et al., 2011). Such an approach is not suitable for smaller earthquakes as the signal to noise ratio is lower and more importantly because the high-frequency signal duration is dominated by the P-wave coda rather than by the source duration. In this case, T_d is defined as a function of magnitude (Fig. 1). This empirical value is efficient to extract the focal mechanism and depth of the earthquake, but may lead to an underestimation of the STF duration (and therefore an underestimation of the moment magnitude), in case of earthquakes longer than expected with respect to their magnitude. That is why at the end of the first step of Fig. 1, we consider a longer time, named T_s, to estimate the moment magnitude. The same time T_s is then used to retrieve the broadband ASTFs (step 2). In the final step, each ASTF is cut to a value T_R ($<T_s$) based on the information provided by the ASTFs stack: the stacking procedure is efficient to reduce the amplitudes of the ASTFs features which are inconsistent between stations and thus to determine the average duration after which the moment release becomes not significant. The ASTF-dependent T_R value is the time at which the ASTF takes very low values in the vicinity of the average duration.

The flowchart of Fig. 1 has been applied to all the events recognized as earthquakes with moment magnitude larger than 5.8 in the NEIC-PDE catalog (http://earthquake.usgs.gov/data/pde.php) since 1992 (~5500 earthquakes between 1992 and 2015). STFs are not available for all these events, for the following reasons, listed from the most common cases to the less ones. (1) Events with not enough stations having a good signal-to-noise ratio, which complicates the determination of their focal mechanism and depth (step 1 in the flowchart). This is often the case for "old" earthquakes in the period 1992–1994 because of the small number of available digital stations; a common case is also the occurrence of a large earthquake in the hours preceding the event to be analyzed. (2) Earthquakes without a sufficient number of good P-wave broadband signals, which does not allow to reliably extract ASTFs (step 2 in the flowchart). This is often the case for strike-slip earthquakes with moderate magnitudes, because of their low radiation coefficients. (3) Complex earthquakes or earthquakes occurring in a complex structure. Complex earthquakes can be events including a significant mechanism change or a large vertical extent. This can affect the step 1, in which case the first-order source parameters cannot be reliably determined, or more commonly the step 2. In this case also, strike-slip earthquakes are more likely to be rejected, because even a small mechanism change has a large effect on the radiation. Complex structure (in particular related to a deep water layer) results in P-wave broadband signals that cannot be reliably deconvolved from the point-source synthetics (step 2). (4) Rare cases related to the duration of the earthquake. The a priori choice of the maximum duration for earthquakes in the magnitude range [5.8–7] (step 1) can lead to rejection of some if they are anomalously long (or composed of several subevents). Large earthquakes (M > 7) should not suffer from this issue, because the duration is empirically determined from the high-frequency P waves (see also Ni et al., 2005). However, extreme events with a duration longer than 200 s cannot be analyzed with the SCARDEC method because of interferences between the main body wave phases: we cannot select in this case a time window where a given body wave is not mixed with another one (when *P*-wave is mixed with *PP*-wave, *PP*-wave is mixed with *PPP*-wave, *PPP*-wave *with S*-wave...). In the period 1992–2015, the only event excluded for this reason is the 2004/12/26 Sumatra earthquake. As a result of these limitations, the STF SCARDEC catalog contains 2782 events between 1992 and 2014/12/31.

The focal mechanism and depth of these earthquakes are shown in the map of Fig. 2. A consistency indicator of the SCARDEC method can be provided by comparing these 1st order source parameters with the ones provided by the Global CMT method (Ekström et al., 2012). Fig. 3a and b shows the comparison for the moment magnitude and depth, respectively, while Fig. 3c shows the comparison for the 6 independent components of the moment tensor. In terms of average differences, observed biases are small. A noticeable one concerns the moment magnitude which is in average 0.02 larger for SCARDEC than for Global CMT. Fig. 3a shows that this difference comes from moderate earthquakes (up to Mw ~ 7). We can attribute it to the complex STF shapes allowed by the SCARDEC method which can lead to larger moment than the simple shapes (boxcars or triangles) imposed by Global CMT.

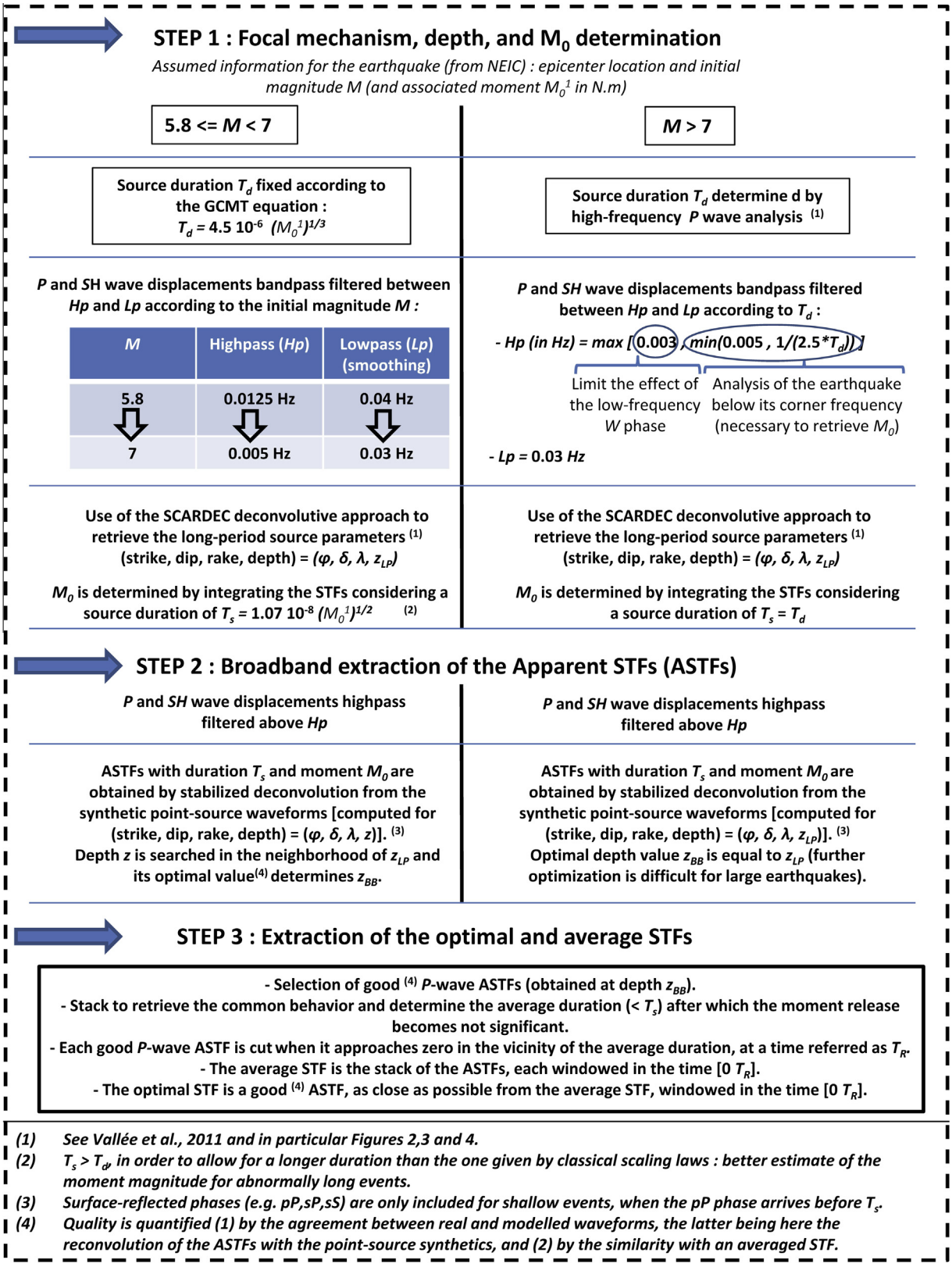

Fig. 1. Flowchart describing the three main steps leading to the extraction of the broadband STFs (average and optimal) together with the 1st order source parameters (depth, moment magnitude and focal mechanism). Note that depending on the magnitude range (larger or smaller than 7), slightly different approaches are followed in steps 1 and 2.

Another reason likely comes from the fact that the SCARDEC method determines depths shallower than the 12 km limit imposed by Global CMT, which results in a larger moment after deconvolution (as the teleseismic radiation is usually less and less efficient when the source approaches the surface). Larger standard error differences for $M_{r\theta}$ and $M_{r\varphi}$, compared to the other moment tensor components, likely come from the joint effect that (1) these components are not well resolved with long period surface waves

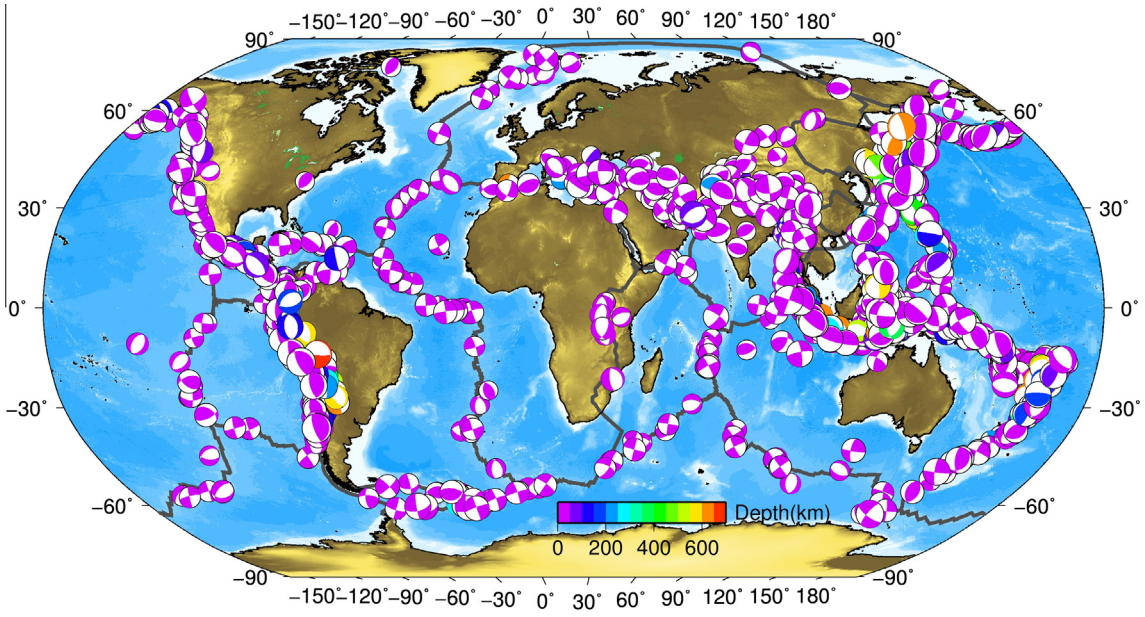

Fig. 2. Map showing all the earthquakes (2782 on 2014/12/31) for which the full SCARDEC information is available (focal mechanism, depth, moment magnitude and STFs). Depth and magnitude control the color and size of the beachball representing the focal mechanism, respectively. Note that large earthquakes are shown in the foreground and frequently hide smaller earthquakes of the same area. All these earthquakes are present in the database available in the webpage *http://scardec.projects.sismo.ipgp.fr*.

for shallow earthquakes (Kanamori and Given, 1981), implying that the resolution power of Global CMT is lower for these components and (2) that in the common case of shallow-dipping thrust or normal earthquakes, body waves methods such as SCARDEC are sensitive to the difference (strike – rake) rather than to each of the parameters separately. This does not affect the components $M_{\theta\theta}$ and $M_{\varphi\varphi}$ – which only depend on the difference (strike – rake), but does affect the $M_{r\theta}$ and $M_{r\varphi}$ components.

Fig. 4 refines the depth comparison shown in Fig. 3b by showing also the differences with the NEIC-PDE hypocentral depth and separating the catalog between shallow and deep earthquakes. The standard errors show that the depth values are less scattered in the SCARDEC-GCMT comparison. They also show that the differences do not statistically increase at shallow depths, the apparent larger scatter being due to the larger number of shallow earthquakes.

As a whole, there is a close agreement between GCMT and SCARDEC approaches, which shows that SCARDEC is able to well retrieve these global source parameters, even if using only body waves. This is a good indication that the point source synthetics (built from earthquake depth and focal mechanism) will allow to retrieve suitable STFs. The agreement in terms of seismic moment ensures that the amplitude of the STFs will not be underestimated, even for very large earthquakes.

3. Characteristics of the STFs provided in the catalog

3.1. Optimal and average STFs

As illustrated in the flowchart of Fig. 1, we make the choice of providing two STFs for each earthquake. The first one is averaged over good-quality P-wave ASTFs, with the goal of robustly extracting the global behavior of the source. The averaging procedure makes the obtained STF insensitive to possible outliers and does not strongly bias the global shape of the STF, because directivity effects remain modest for teleseismic P waves, in particular in the most common cases of near-horizontal rupture propagation. However, averaging always tends to reduce the high frequency content, which can for example perturb spectral analyses of the STFs. That is why we also provide one of the ASTFs as the optimal STF, based on the two following criteria: (1) being a good ASTF, in the sense that its convolution with the point-source synthetics gives close agreement with the observed waveforms and (2) being close to the averaged STF in order to limit the risk of providing an outlier as the optimal STF.

3.2. Examples

We provide here the information given by the SCARDEC method for three illustrative shallow earthquakes of different magnitudes and focal mechanisms. The first one (Fig. 5a) is the L'Aquila earthquake (Central Italy, 06 April 2009, Mw = 6.3). Its shallow extensive mechanism is well determined by SCARDEC (strike/dip/rake = 128°/50°/−103°, depth = 6 km). The light grey curves show all the good P-wave ASTFs which have been used to obtain the average STF shown by the thick grey curve. As expected, details of the ASTFs differ, but they all show the same global behavior, with a global duration of 8–10 s and a peak moment rate of 5–$7{\cdot}10^{17}$ Nm/s. This is in very good agreement with STFs provided by studies complementing the teleseismic data with local and geodetic data (Balestra and Delouis, 2015). The black curve is the "optimal" ASTF (the closest from the average STF) which captures some local complexities better than the average STF.

The second example (Fig. 5b) is the Hector Mine earthquake (California, 16 October 1999, Mw = 7.1). Its strike-slip mechanism (strike/dip/rake = 336°/80°/173°) is at the origin of the larger variability observed for the ASTFs. Indeed, a degree of non-planarity of the geometry is likely present in most earthquakes but this feature is much more critical for strike-slip earthquakes as it strongly affects the teleseismic radiation. In the case of the Hector Mine earthquake, the variation of the fault azimuth is clearly imaged by detailed studies (e.g. Salichon et al., 2004). Variability of the ASTFs results in a larger difference between the average and optimal STFs. However, it does not prevent robust extraction of the main characteristics of the earthquake in terms of peak-moment rate and global duration.

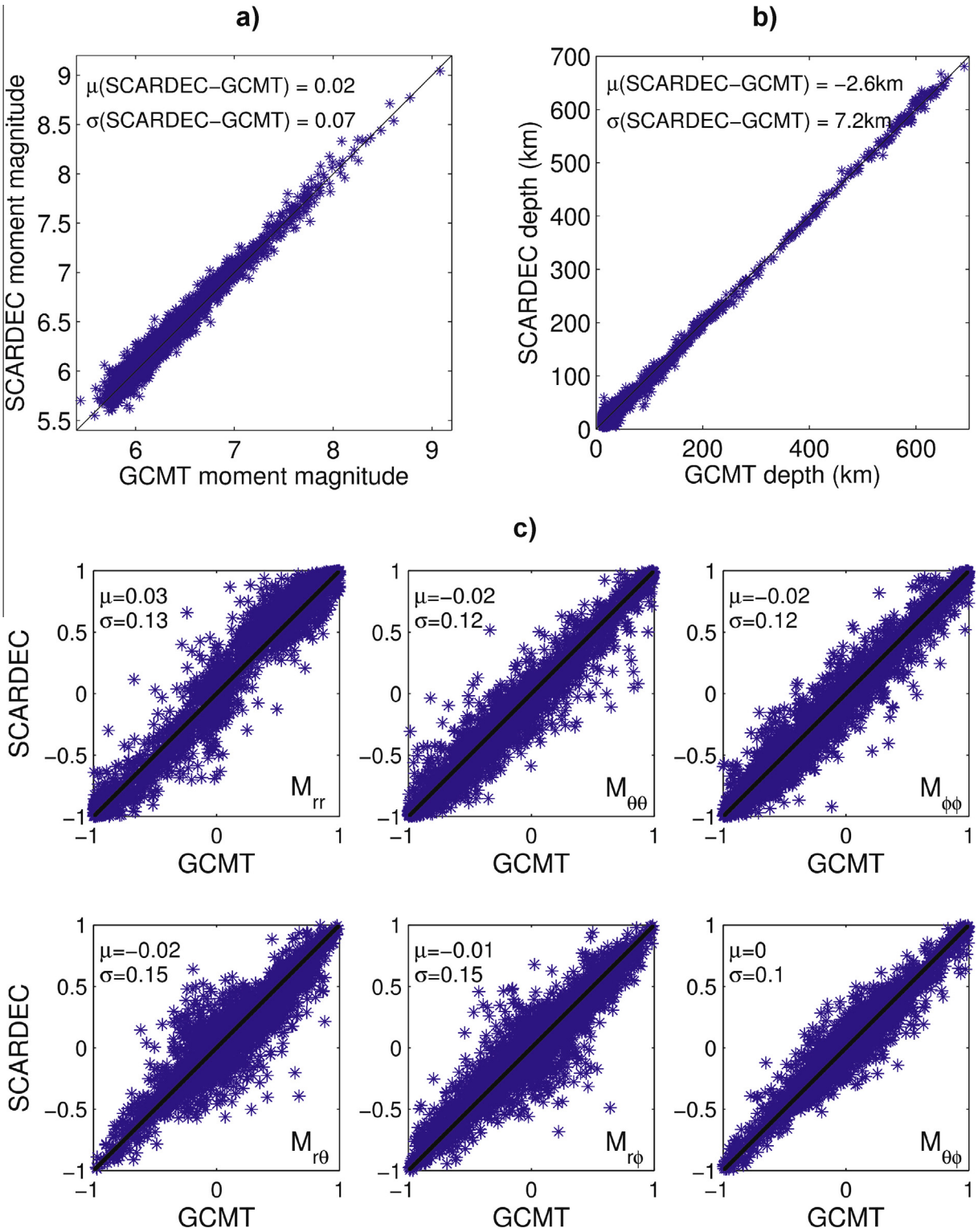

Fig. 3. Comparison between SCARDEC and Global CMT source parameters, showing the average differences (μ) and standard errors (σ). (a) Moment magnitude; as already emphasized in the article describing the SCARDEC method (Vallée et al., 2011), there is no underestimation at very large magnitudes. (b) Depth. (c) Moment tensor components, in the Global CMT formalism. The values indicated for Global CMT are the ones related to the best double couple solution.

The last example is given for a very large subduction earthquake, in order to illustrate the ability of the procedure of providing meaningful STFs, even for events with large spatial extent: the earthquake shown in Fig. 5c is the Arequipa earthquake (Peru, 23 June 2001, Mw = 8.4), which propagated for 150–200 km along the subduction trench (Bilek and Ruff, 2002). The selected ASTFs show some variability related to directivity effects, but do not prevent the extraction of a meaningful average (thick grey curve). The optimal ASTFs (black curve) obtained in this case tends to be a non-directive ASTF, as it is chosen as close as possible from the average STF.

We also give in Fig. 6 an illustration of the variability of the STFs for large earthquakes. The selection includes all the shallow sub-

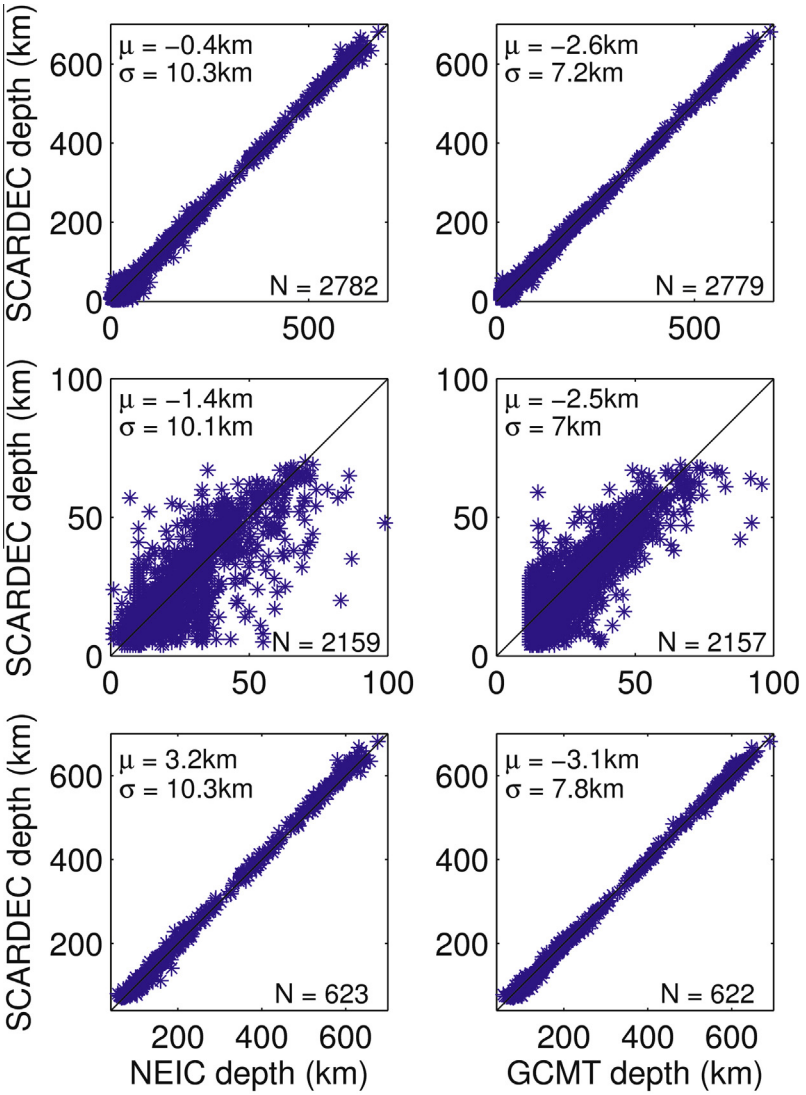

Fig. 4. Comparisons between SCARDEC, NEIC-PDE and GCMT depth determinations. (Left) Comparison between SCARDEC and NEIC-PDE depths, showing the average differences (μ), standard errors (σ) and the number of earthquakes considered (N); top, middle and bottom subfigures are for the whole catalog, shallow earthquakes (depth <70 km) and deep earthquakes (depth >70 km), respectively. (Right) Same as in the left column, but for the comparison between SCARDEC and GCMT depths.

duction earthquakes of the Sumatra-Java trench with moment magnitude in the range [7.2–8.5] (since 2000). The Global CMT parametrized STFs (boxcar or triangle) are also indicated. This figure shows that some earthquakes closely follow what is expected by the standard scaling laws assumed by Global CMT (for example the 2008/02/20 earthquake) while other significantly differ. The most spectacular case is the 2006/07/17 Java earthquake, which is a well-known "tsunami" earthquake (Ammon et al., 2006), with a very long duration and low moment rate relative to its magnitude. Such departures from the scaling laws are useful both for theoretical understanding of the earthquake diversity and for seismic hazard related studies.

3.3. Limitations

Optimal and average STFs can be used for various applications, in the fields of source or structure seismology. In a number of cases, it would be useful to precisely know the reference time of the beginning of the STF. At first order, the 0 time of the STFs (see the examples in Fig. 5) is the NEIC-PDE hypocentral time of the earthquake. However, differences up to a few seconds are expected, for the following reasons: (1) SCARDEC method determines the depth of the earthquake, which can be different from the original NEIC-PDE depth. In this case, the hypocentral time should be recalculated taking into account the depth difference. (2) Because the beginning times of the ASTFs are predicted in a spherical model, ASTFs can be misaligned one compared to the other up to a few seconds (for P waves). When computing the average STF, we allow for an optimal time shift for each ASTF based on the maximum correlation between ASTFs. Finally, the 0 time is fixed at the beginning of the first significant moment release of the optimal STF. In case of impulsive and well distributed ASTFs, we expect this procedure to provide a 0 time very close to the NEIC-PDE origin time of the earthquake. However some differences (up to a few seconds, on the same order of the uncertainty of the P arrival times) may occur in case of slow initial moment release. When using STFs of the catalog, we therefore encourage procedures which take into account this uncertainty of the reference time.

The SCARDEC deconvolutive approach is able to retrieve complex ASTFs with several episodes of moment release. However, in the late parts of the STFs, it is important to well separate real source effects from spurious moment episodes related to unmodeled seismic phases. As the latter effect tends to result in incoherent signals between distant stations, their amplitudes are reduced

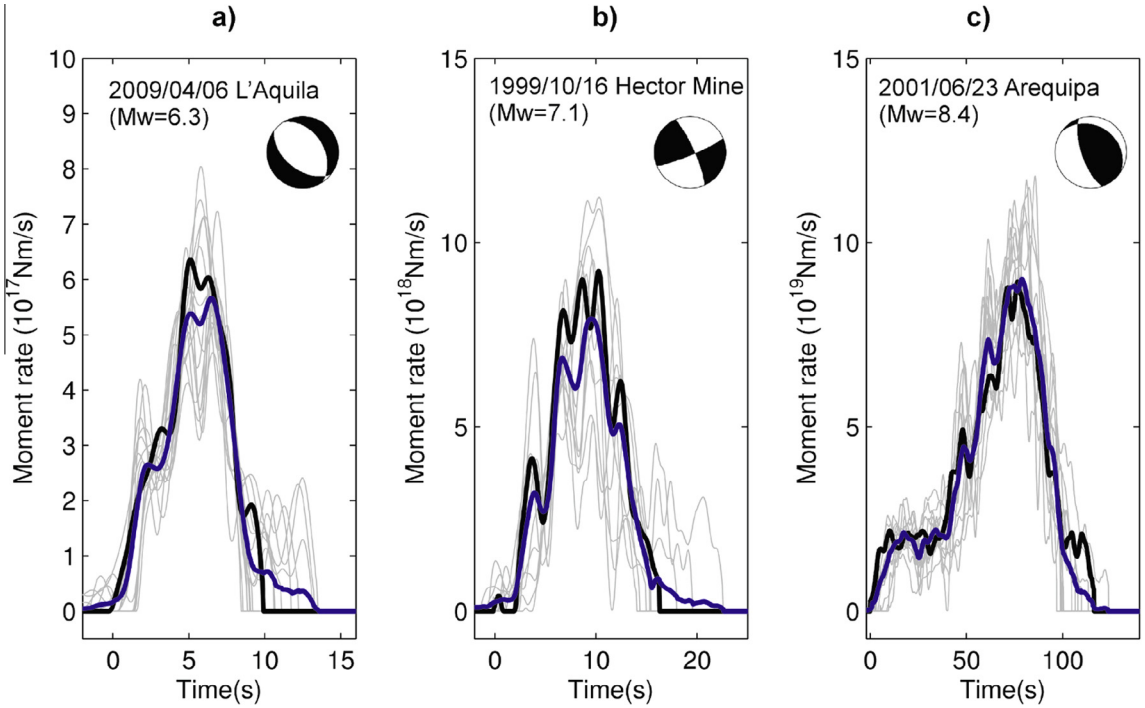

Fig. 5. ASTFs, optimal and average STFs for three earthquakes with different magnitudes and seismo-tectonic contexts. For the three events, ASTFs, average and optimal STFs are shown with light grey, thick grey and black colors, respectively.

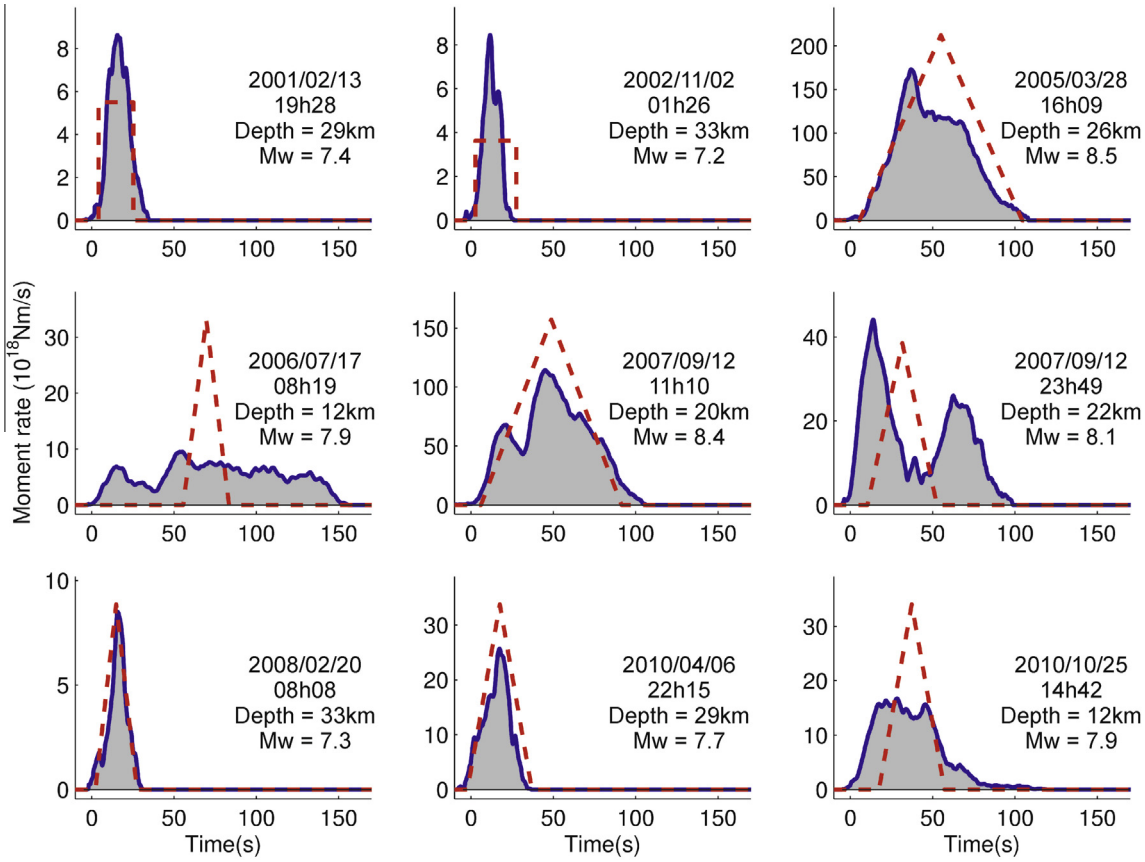

Fig. 6. Variability of STFs for large earthquakes. Shallow (depth <40 km) subduction earthquakes of the Sumatra-Java trench in the magnitude range [7.2–9], since 2000, are shown in this figure. The average SCARDEC STFs are filled with grey. The GCMT parametrized STFs (boxcar or triangle) are shown with dashed lines.

in the average STF. We therefore use a criterion on the average STF, based on the amplitude of the late local STF maxima compared to the absolute maximum, to determine the end of the STFs. STFs are typically cut after the last maximum reaching 40% of the absolute one. This approach implies that late minor source emissions will be lost but it reduces the risk of introducing structure-related effects in the STFs. Observation of the STF database shows that this procedure limits the existence of such spurious effects to some configurations where P-wave coda is strong and coherent, the most common cases being offshore strike-slip events. In these cases, long and complex STFs can be questioned, and further interpretation requires analysis of the original P-wave signals.

The fact of providing two STFs (optimal and average) for each earthquake also provides a way to estimate the quality of the STFs. In cases where ASTFs are precisely determined for most of the stations, we expect them to be close to each other (only perturbed by minor directivity effects), which implies that the average and the optimal STF are themselves close to each other. More caution should be taken when these two functions significantly differ, as it occurs when the ASTFs are likely too different to be explained by directivity effects. The most common case is a variation of the focal mechanism during the earthquake, which cannot be taken into account in the deconvolution. This results in modifications of the shape and amplitude of the ASTFs, not representative of the moment rate. As already mentioned, this configuration is much more common for strike-slip earthquakes than for dip-slip earthquakes, because in the first case, even a slight mechanism variation results in a large change of the teleseismic amplitudes.

Finally, as in all teleseismic analyses (e.g. GCMT), it is difficult to determine how shallow an earthquake is, in particular for dip-slip mechanisms. In the latter case, we fix the minimal depth at 6 km for events close to magnitude 6 and increase this value up to 12 km for large earthquakes (magnitude 7 and above). Shallow depths are indeed better resolved when source durations are short, which limits the interaction between direct and surface-reflected phases. For strike-slip earthquakes, depths down to 4 km are allowed. When depth approaches the above limits, direct interpretation of its value should be avoided, and other data types should be used to determine how close the earthquake actually is to the surface.

4. Description of the access to the database

The source parameters determined by the SCARDEC method (STFs, as well as the depth, moment magnitude and focal mechanism) for all the earthquakes of the database are made available through the webpage *http://scardec.projects.sismo.ipgp.fr*. This page offers a multi-criteria search (date, epicentral location, depth, magnitude, depth, focal mechanism parameters) in order to easily select the desired earthquakes. For each earthquake meeting these criteria, the STFs (optimal and average) can be seen online. The selected STFs can also be downloaded in a simple format where the first two lines of each STF file provide the source parameters (epicentral location and origin time from NEIC-PDE; depth, seismic moment, focal mechanism from SCARDEC), and all the other lines the STF (two columns with time and moment rate). For each earthquake, two such files corresponding to the optimal and average STFs are provided. For exhaustive analyses or studies requiring other selection criteria, we also provide access to the whole database. As of now, the database is complete from 1992 to 2014/12/31 and contains 2782 earthquakes. We plan to update it in the future on a regular basis.

We hope that this STF database will be useful to the seismological community. Applications are expected to be various, as STFs offer quantitative information on the source process, helping fundamental research on earthquake mechanics or more applied studies related to seismic hazard. On the other hand, they can be also seen as a tool for Earth structure analyses, where the excitation of the medium at the source has to be known.

Acknowledgments

We are grateful to the global broadband seismic network, in particular to the arrays IU, G (GEOSCOPE), II, GE (GEOFON), IC and GT for high-quality data and public access to the continuous waveforms. Data have been retrieved through the IRIS (http://www.iris.edu/hq/) and GEOSCOPE (http://geoscope.ipgp.fr/index.php/en/) data centers, with the 'breq_fast' (https://ds.iris.edu/ds/nodes/dmc/manuals/breq_fast/) and 'arclink' (http://www.seiscomp3.org/wiki/doc/applications/arclink) protocols, respectively. This study has been supported by the IFMORE project (AO INSU ALEAS 2014). Most numerical computations were performed on the S-CAPAD platform, IPGP, France. We thank Michel Lecocq for configuring the machine dedicated to STFs requests, Arthur Delorme for his expertise in mapping tools, and Agnès Chounet for her comments on the STFs request web tool. This is IPGP contribution number 3751. The authors thank two anonymous reviewers for their comments that helped improve the manuscript.

References

Aki, K., 1967. Scaling law of seismic spectrum. J. Geophys. Res. 72, 1217–1231.
Aki, K., 1972. Scaling law of earthquake source time function. Geophys. J. R. Astron. Soc. 31, 3–25.
Allmann, B.P., Shearer, P.M., 2009. Global variations of stress drop for moderate to large earthquakes. J. Geophys. Res. 114, B01310.
Ammon, C.J., Kanamori, H., Lay, T., Velasco, A.A., 2006. The 17 July 2006 Java tsunami earthquake. Geophys. Res. Lett. 33, L24308.
Anderson, D., Minster, J., 1979. The frequency dependence of Q in the Earth and implications for mantle rheology and Chandler wobble. Geophys. J. R. Astron. Soc. 58, 431–440.
Balestra, J., Delouis, B., 2015. Reassessing the rupture process of the 2009 L'Aquila Earthquake (Mw 6.3) on the Paganica fault and investigating the possibility of coseismic motion on secondary faults. Bull. Seismol. Soc. Am. 105, 1517–1539.
Baltay, A.S., Hanks, T.C., Beroza, G.C., 2013. Stable stress-drop measurements and their variability: implications for ground-motion prediction. Bull. Seismol. Soc. Am. 103, 211–222.
Bilek, S.L., Lay, T., 1999. Rigidity variations with depth along interplate megathrust faults in subduction zones. Nature 400, 443–446.
Bilek, S.L., Ruff, L.J., 2002. Analysis of the June 23, 2001 Mw = 8.4 Peru underthrusting earthquake and its aftershocks. Geophys. Res. Lett. 29, 1960.
Boatwright, J., 1984. Seismic estimates of stress release. J. Geophys. Res. 89, 6961–6968.
Bouchon, M., 1976. Teleseismic body wave radiation from a seismic source in a layered medium. Geophys. J. R. Astron. Soc. 47, 515–530.
Brune, J.N., 1970. Tectonic stress and the spectra of seismic shear waves from earthquakes. J. Geophys. Res. 75, 4997–5009.
Choy, G.L., Cormier, V.F., 1986. Direct measurement of the mantle attenuation operator from broadband P and S waves. J. Geophys. Res. 91, 7326–7342.
Cotton, F., Archuleta, R., Causse, M., 2013. What is sigma of stress drop? Seismol. Res. Lett. 84, 42–48.
Courboulex, F., Vallée, M., Causse, M., Chounet, A., 2016. Stress-drop variability of shallow earthquakes extracted from a global database of source time functions. Seismol. Res. Lett. http://dx.doi.org/10.1785/0220150283.
Der, Z.A., 1998. High-frequency P- and S-wave attenuation in the Earth. Pure Appl. Geophys. 153, 273–310.
Dziewonski, A.M., Anderson, D.L., 1981. Preliminary reference Earth model. Phys. Earth Planet. Inter. 25, 297–356.
Ekström, G., Nettles, M., Dziewonski, A.M., 2012. The global CMT project 2004–2010: centroid-moment tensors for 13,017 earthquakes. Phys. Earth Planet. Inter. 200–201, 1–9.
Garcia, R.F., Schardong, L., Chevrot, S., 2013. A nonlinear method to estimate source parameters, amplitude, and travel times of teleseismic body waves. Bull. Seismol. Soc. Am. 103, 268–282.
Hosseini, K., Sigloch, K., 2015. Multifrequency measurements of core-diffracted P waves (Pdiff) for global waveform tomography. Geophys. J. Int. 203, 506–521.
Houston, H., 2001. Influence of depth, focal mechanism, and tectonic setting on the shape and duration of earthquake source time functions. J. Geophys. Res. 106, 11137–11150.
Kanamori, H., 1972. Mechanism of tsunami earthquakes. Phys. Earth Planet. Inter. 6, 346–359.

Kanamori, H., Given, J.W., 1981. Use of long-period surface waves for rapid determination of earthquake source parameters. Phys. Earth Planet. Inter. 27, 8–31.
Kennett, B.L.N., Engdahl, E.R., 1991. Travel times for global earthquake location and phase association. Geophys. J. Int. 105, 429–465.
Lentas, K., Ferreira, A.M.G., Vallée, M., 2013. Assessment of SCARDEC source parameters of global large (Mw ⩾ 7.5) subduction earthquakes. Geophys. J. Int. 195, 1989–2004.
Margaris, B.N., Hatzidimitriou, P.M., 2002. Source spectral scaling and stress release estimates using strong-motion records in Greece. Bull. Seismol. Soc. Am. 92, 1040–1059.
Müller, G., 1985. The reflectivity method: a tutorial. J. Geophys. 58, 153–174.
Ni, S., Kanamori, H., Helmberger, D., 2005. Energy radiation from the Sumatra earthquake. Nature 434, 582–582.
Salichon, J., Lundgren, P., Delouis, B., Giardini, D., 2004. Slip history of the 1999, October 16, Mw = 7.1, Hector Mine earthquake (California) from the inversion of InSAR, GPS and teleseismic data. Bull. Seismol. Soc. Am. 94, 2015–2027.
Sigloch, K., Nolet, G., 2006. Measuring finite-frequency body-wave amplitudes and traveltimes. Geophys. J. Int. 167, 271–287.
Stähler, S.C., Sigloch, K., 2014. Fully probabilistic seismic source inversion – Part 1: Efficient parameterisation. Solid Earth 5, 1055–1069.
Tanioka, Y., Ruff, L., 1997. Source time functions. Seismol. Res. Lett. 68, 386–400.
Tocheport, A., Rivera, L., Chevrot, S., 2007. A systematic study of source time functions and moment tensors of intermediate and deep earthquakes. J. Geophys. Res. 112, B07311.
Vallée, M., 2013. Source time function properties indicate a strain drop independent of earthquake depth and magnitude. Nat. Commun. http://dx.doi.org/10.1038/ncomms3606.
Vallée, M., Charléty, J., Ferreira, A.M.G., Delouis, B., Vergoz, J., 2011. SCARDEC: a new technique for the rapid determination of seismic moment magnitude, focal mechanism and source time functions for large earthquakes using body wave deconvolution. Geophys. J. Int. 184, 338–358.
Vassiliou, M.S., Kanamori, H., 1982. The energy release in earthquakes. Bull. Seismol. Soc. Am. 72, 371–387.